

*Full paper*

## **Computational Simulation of the Adsorption Behavior of Benzimidazolone Derivatives as Inhibitors for Ordinary Steel Corrosion in HCl 1M**

**Abdeslam El Assry,<sup>1</sup> M'Hamed Touil,<sup>2</sup> Fouad Benhiba,<sup>3,4</sup> Bouziane Benali,<sup>5</sup> Hassan Rabaâ,<sup>2</sup> Brahim Lakhri,<sup>6</sup> Ismail Warad,<sup>7</sup> Fouad Bentiss,<sup>8</sup> and Abdelkader Zarrouk<sup>4,\*</sup>**

<sup>1</sup>*Laboratory of Polymer Physics and Critical Phenomena, Department of Physics, Faculty of Sciences Ben M'Sik, Hassan II University, Casablanca, Morocco*

<sup>2</sup>*ESCTM (PCMVC Laboratory), Faculty of Sciences, Ibn Tofail University, P.O. Box 133, Kenitra 14000, Morocco*

<sup>3</sup>*Laboratory of Separation Processes, Faculty of Sciences, IbnTofail University, P.O. Box 133, 14000, Kenitra, Morocco*

<sup>4</sup>*Laboratory of Materials, Nanotechnology and Environment, Faculty of Sciences, Mohammed V University, Av. Ibn Battouta, P.O. Box 1014, Agdal-Rabat, Morocco*

<sup>5</sup>*Laboratory of Optoelectronic, Physical Chemistry of Materials and Environment, Department of Physics, Faculty of Sciences, Ibn Tofail University, PB. 133, 1400, Kenitra, Morocco*

<sup>6</sup>*Laboratory of Agro-Resources, Polymers and Process Engineering, Faculty of Sciences, Ibn Tofail University, PO Box 133, 14000, Kenitra, Morocco*

<sup>7</sup>*Department of Chemistry and Earth Sciences, PO Box 2713, Qatar University, Doha, Qatar*

<sup>8</sup>*Laboratoire de Catalyse et de Corrosion des Matériaux (LCCM), Faculté des Sciences, Université Chouaib Doukkali, B.P. 20, M-24000 El Jadida, Morocco*

\*Corresponding Author, Tel.: +212 665 201 397; Fax: +212 537 774 261

E-Mail: [azarrouk@gmail.com](mailto:azarrouk@gmail.com)

*Received: 4 February 2020 / Received in revised form: 16 May 2020 /*

*Accepted: 18 May 2020 / Published online: 31 May 2020*

---

**Abstract-** The adsorption behavior of Benzimidazol-2-one (Bz), 5-Methylbenzimidazol-2-one (CH<sub>3</sub>Bz) and 5-Chlorobenzimidazol-2-one (ClBz) as inhibitors for mild steel corrosion in HCl 1M have been studied computationally using density functional theory (DFT) calculations with the hybrid B3LYP functional. The calculations were focused on the protonated forms of the molecules under study, seeing that these classes of inhibitors can easily be protonated in acidic medium. The most preferred protonation centers were determined proton affinity (PA). Fukui indices have been computed to evaluate the nucleophilic and electrophilic sites of atoms in the molecule. The interaction of the inhibitors with the iron surface was studied by calculating the combined energy ( $E_{com}$ ) and the free energy of adsorption ( $\Delta G_{ads}^{\circ}$ ). Observable correlation was found between experimental corrosion inhibition efficiency and the theoretical data. The molecular dynamics (MD) and Monte Carlo (MC) simulations used show that all investigated Benzimidazol inhibitors are positioned parallel to the metal surface reflecting the coverage of a large portion of the steel surface.

**Keywords-** Ordinary steel; Benzimidazolone; Adsorption; Density functional theory; Monte Carlo; Molecular dynamics

---

## 1. INTRODUCTION

Many classes of organic compounds are widely used as corrosion inhibitors [1-8]. Ordinary steel is broadly used in various industrial operations, especially, in petroleum industries and power plants [9]. These industries occurs in environments in which, acids are broadly used for pickling, cleaning acid, acidification of oil wells and other applications, allowing acid corrosion to take place. In this regard, several organic chemicals have been used to effectively protect metals and alloys against corrosion problems. Mainly, heterocyclic compounds restrain heteroatoms such as S, N & O organic compounds, it has been proven that among the most effective inhibitors corrosion against in acidic environment [10-13]. Inhibiting action is usually explained by the formation of film on the metal surface based on D-A interactions among  $\pi$ -electrons of the aromatic ring or among unshared electron pairs of heteroatoms and vacant d-orbitals of surface iron atoms [14-16]. Among the various compounds studied with nitrogen atoms as inhibitors, benzimidazolones are regarded as beneficial to the environment. A study of the thermal, spectral and structural of the benzimidazolone has been recently reported by our group [17-20]. In addition, several works have reported that heterocyclic molecules based on benzimidazolones showing various applications in various domains such as analytical chemistry, medicine and agrochemistry [21,22]. From these advantages, we performed a study on the three benzimidazolone derivatives such as benzimidazol-2-one (Bz), 5-methylbenzimidazol-2-one (CH<sub>3</sub>Bz) and 5-chlorobenzimidazol-2-one (ClBz). The experimental inhibitive property of three organic compounds has been reported by our group.

The phenomenon of corrosion inhibition is very complex enough, and several factors of

influence such as electrodes, distilled water, aggressive species, etc. can lead to more or less different results. It is crucial, therefore, to use a supplementary approach such as DFT and molecular simulations which are based on the minimum of the factors. The DFT method makes it possible to study the behaviour of the electronic structure in order to evaluate the chemical reactivity of an organic molecule. Monte Carlo (MC) and molecular dynamics (MD) simulations seem to best meet the requirements mentioned above, as well as the presence of solvent and metal substrate [23,24]. All this with radial distribution function (RDF) and mean squared displacement (MSD) were used to provide additional information on the reaction mechanism of an inhibitor in relation to the surface of steel. The purpose of this study is correlating the corrosion inhibition activity with the chemical properties/descriptors of three molecules conformed by the radical of nucleophilic and electrophilic substitutions (H, Cl, CH<sub>3</sub>) in cyclohexane of Benzimidazolone (Fig. 1), to determine the action modes and the adsorption mechanisms of our compounds on the metallic surface.

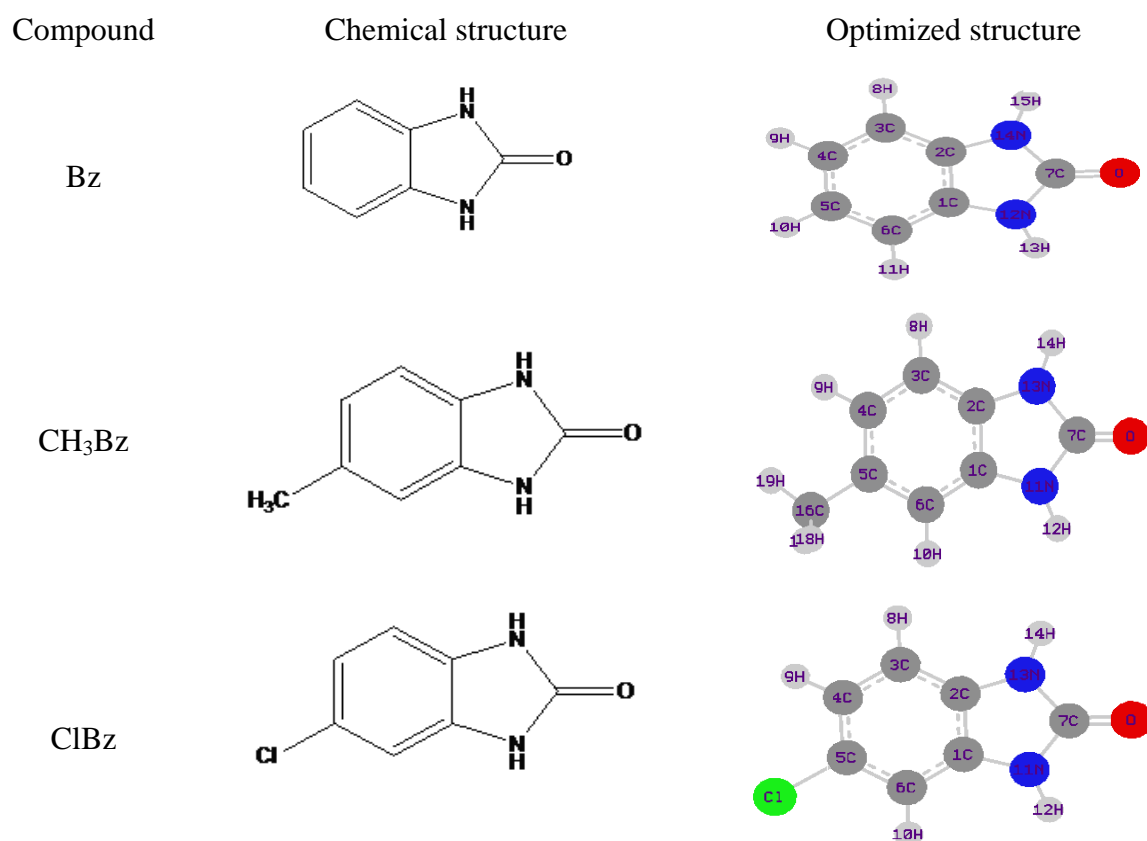


**Fig. 1.** Chemical and optimized structures of Benzimidazolone and its derivatives

## 2. Methodology

### 2.1. DFT

Composed parameters were optimized by using DFT calculations with the hybrid B3LYP functional and 6-31+G(d,p) Gaussian basis sets [25,26], comprising the  $E_{\text{HOMO}}$ , the  $E_{\text{LUMO}}$ ,

LUMO- HOMO energy gap ( $\Delta E$ ), dipole moment ( $\mu$ ), molecular volume ( $V_i$ ), total negatives charges (TNC), total energy (TE), isotropic polarizability  $\langle\alpha\rangle$  and anisotropic polarizability ( $\Delta\alpha$ ), have been correlated to experimental results. The adsorption of the inhibitors compounds on iron surfaces was studied using one iron atom.  $E_{com}$  was calculated to assess the stability of the complex (Inhibitor-Fe). The adsorption mechanism, the standard free energy of adsorption  $\Delta G_{ads}^\circ$  was computed to provide the best description.

## 2.2. Molecular dynamics (MD) and Monte Carlo (MC) simulations

Recently, MD and MC simulations have known gaining great importance in corrosion inhibition studies [27]. This method of simulation is used frequently to better understand the interaction and adsorption of an inhibitory molecule on the surface of the substrate [28]. In the present work, our system studied containing  $5H_3O^+$ ,  $5Cl^-$  and  $500H_2O$  and one monomer of tested molecule was effectively constructed. The simulations were carried out using for cite code of Materials Studio 8 software package [29]. In the simulation part, Cell parameters  $a = 32.27 \text{ \AA}$ ,  $b = 32.27 \text{ \AA}$  and  $c = 30.13 \text{ \AA}$  size,  $(13 \times 13)$  unit cell and  $40 \text{ \AA}$  vacuum with periodic boundary condition. The structures of the Bz,  $CH_3Bz$  and  $ClBz$  compounds are pre-optimized using with the GGA (Generalized Gradient Approximation) and DNP (Dual Numerical Polarization) functions. Dynamics run parameter are NVT ensemble with Andersen control method [30]. After 400000 the number of steps with 400ps duration, the system reaches equilibrium which explains that both the energy and temperature reach equilibrium. MD simulation was performed by using COMPASS force field [31]. Dynamics run parameter are NVT ensemble, spline width  $1 \text{ \AA}$ , cutoff distance  $15.5 \text{ \AA}$  and buffer width  $0.5 \text{ \AA}$ .

The interaction ( $E_{interaction}$ ) and binding ( $E_{binding}$ ) energies of our system are calculated according to the following equations [32]:

$$E_{interaction} = E_{total} + E_{solution} - E_{surface+solution} - E_{inhibitor+solution} \quad (1)$$

$$E_{binding} = -E_{interaction} \quad (2)$$

where  $E_{total}$  is the total energy of the whole studied system,  $E_{surface+solution}$  is referred to the total energy of Fe (110) surface and solution without the inhibitor and  $E_{inhibitor+solution}$  represents the total energy of inhibitor and solution, and  $E_{solution}$  is the total energy of the solution.

## 3. RESULT AND DISCUSSION

### 3.1. Theoretical models relevant to analyze drug-drug and drug-DNA interactions in cyclic voltammetry

The rate of corrosion ( $W_{corr}$ ) of steel in 1M HCl medium containing various quantities of

the benzimidazolones was obtained after immersion of different concentrations of the studied inhibitors during 24 h at  $298 \pm 1$  K. The inhibition performance ( $E_w$  %) in the weight loss (WL) process obtained by:

$$E_w (\%) = \left( 1 - \frac{W_{corr}^i}{W_{corr}^o} \right) \times 100 \quad (3)$$

$W_{corr}^o$  and  $W_{corr}^i$  are the corrosion rates of steel specimens in the without and with of the organic molecules, respectively.

Table 1 presents the  $W_{corr}$  (mg/cm<sup>2</sup>h), and the  $E_w$  % of corrosion of steel in 1 M HCl medium by various concentrations of Bz, CH<sub>3</sub>Bz, and ClBz, as determined by WL after 24 hours. It is very clear that the results obtained in Table 1 show that the presence of Bz, CH<sub>3</sub>Bz and ClBz leads to a decrease in corrosion rate. This is very noticeable at the  $E_w$  % of inhibitory molecules increase with concentration. For high concentrations of inhibitors, we found 38 % for Bz, 77 % for CH<sub>3</sub>Bz, and 87 % for ClBz at  $10^{-3}$  M. These molecules effectively inhibited corrosion of the substrate studied in HCl 1 M, ClBz is the best inhibitor. The order of inhibitory performance of these organic compounds is increased in the following sequence: Bz < CH<sub>3</sub>Bz < ClBz.

**Table 1.**  $E_w$  % of substrate in 1 M HCl solution by different concentrations of Bz, CH<sub>3</sub>Bz, and ClBz

Medium	Witness	Bz	CH <sub>3</sub> Bz	ClBz
Corrosion rate (mg/cm <sup>2</sup> h)	0.137	0.085	0.031	0.018
$E_w$ (%) (24 h)	—	38	77	87

Examination of Table 1 shows that ClBz has better efficiency than other compounds. This may have a connection with the chemical structure of molecules because the substitution of Cl by CH<sub>3</sub> or hydrogen significantly affects the inhibitory efficiency of mild steel in 1 M HCl medium.

This can be explained by the electronic effect. Indeed, chlorine being an electron donor with a mesomeric (M) contributing to an increase of the electron density (load) in the aromatic ring of the compounds. This effect can be justified by the conjunction of the molecule favors the adsorption of the compounds on the metal surface. CH<sub>3</sub> group also gives electrons by an inductive effect, which allows the compounds to adsorb better to the metal surface compared to the case of the substitution of Cl by a proton.

Table 2 reports the inhibitory efficacy for some of the imidazole derivatives recently used as corrosion inhibitors of mild steel in 1 M HCl compared to the newer compounds used in this work.

**Table 2.** Inhibitors performance of benzimidazole derivatives used as corrosion inhibitors in 1 M HCl medium

Inhibitory molecule	Highest inhibition efficiency (%)	Metal exposed	Ref.
2-Aminomethyl benzimidazole	79.4	Mild steel	[33]
2-(Chloromethyl)benzimidazole	81.0	Mild steel	[34]
2-(2-Nitrophenyl)benzimidazole (2NPBI)	87.8	Mild steel	[35]

### 3.2. DFT

#### 3.2.1. Theoretical study of neutral inhibitors

The electrochemical corrosion phenomenon in acidic medium occurs in the liquid phase, and it is well known that the inhibitory molecules in medium act otherwise than in a vacuum, this is why, it is relevant to enclose the solvent effect in the computations. The solvent effect on the compound structure of solute could be studied by a model, which is known as PCM [12]. We have chosen the conductor polarizable calculation model (CPCM) implemented in Gaussian 03 program. So, in order to comprehend the experimental data, the neutral inhibitors states of the surfactant compounds were studied computationally and the quantum chemical parameters/descriptors most relevant to their potential action as corrosion inhibitors was calculated in aqueous phase. The calculated quantum chemical parameters/descriptors of the neutral compounds in aqueous phase are given in Table 3.

High  $E_{\text{HOMO}}$  indicate that the compounds have a tendency to donate electrons to appropriate acceptor compounds with low energy empty molecular orbital [36,37]. Increasing  $E_{\text{HOMO}}$  facilitate adsorption by influencing the transport process through the adsorbed layer. On the other hand,  $E_{\text{LUMO}}$  indicates the ability of accepting electrons to compounds. The lower the value of  $E_{\text{LUMO}}$ , the more probable, that the compounds would accept electrons [38]. That fact may prove that the feedback bonds will be able to be formed among d-orbitals of steel and inhibitor compounds. Training of feedback bonds increases the chemical adsorption of inhibitor compounds on the steel surface [36,39], and so increases the inhibition efficiency. Larger values of energy gap  $\Delta E$  imply more stability for the compounds in reactions [40] and smaller values indicates that the compounds are the more probable to give higher inhibition efficiency. From the Table 3, the  $E_{\text{LUMO}}$  of this class of inhibitors increases in the order ClBz > CH<sub>3</sub>Bz > Bz, this is in good correlation with the experimental data, this, proves that these inhibitors can accept electrons from the metal surface. Also, ClBz has the smallest  $\Delta E = E_{\text{LUMO}} - E_{\text{HOMO}}$  (5.267 eV) compared with other compounds. One might expect that ClBz molecule has a greater tendency to adsorb on metal surface than other compounds, which is a good correlation with the experimental inhibition efficiency.

**Table 3.** The theoretical parameters for Bz, CH<sub>3</sub>Bz and ClBz in the neutral form

Quantum chemical properties/descriptors	Bz	CH <sub>3</sub> Bz	ClBz
E <sub>HOMO</sub> (eV)	-5.973	-5.864	-6.061
E <sub>LUMO</sub> (eV)	-0.545	-0.570	-0.794
ΔE (eV)	5.428	5.294	5.267
μ (Debye)	4.576	4.954	2.416
V <sub>i</sub> (cm <sup>3</sup> /M)	96.16	99.03	115.11
<α> (u.a.)	140.02	155.89	158.55
α (u.a.)	113.980	121.545	139.771
TNC (e)	-3.117	-3.600	-2.929
TE (eV)	-12313.758	-13377.790	-24759.977

Otherwise, μ, TNC, V<sub>i</sub>, <α> and Δα were calculated in aqueous phase, for more report on reactivity of compounds under study. These parameters are closely responsible for the physical adsorption. This last, results of electrostatic interaction among the charged centers of compounds and charged metal surface which results in a dipole interaction of compounds and metal surface. Dipole moment is measure of asymmetry in the molecular charge distribution and the polarity of the polar covalent bond, thus, the high dipole moment probably increases the adsorption among chemical molecule and metal surface [41-43]. The electrons distribution determined by:

$$\alpha = \left( \frac{\partial^2 E}{\partial F_a \partial F_b} \right) \quad \text{a, b : in space} \quad (4)$$

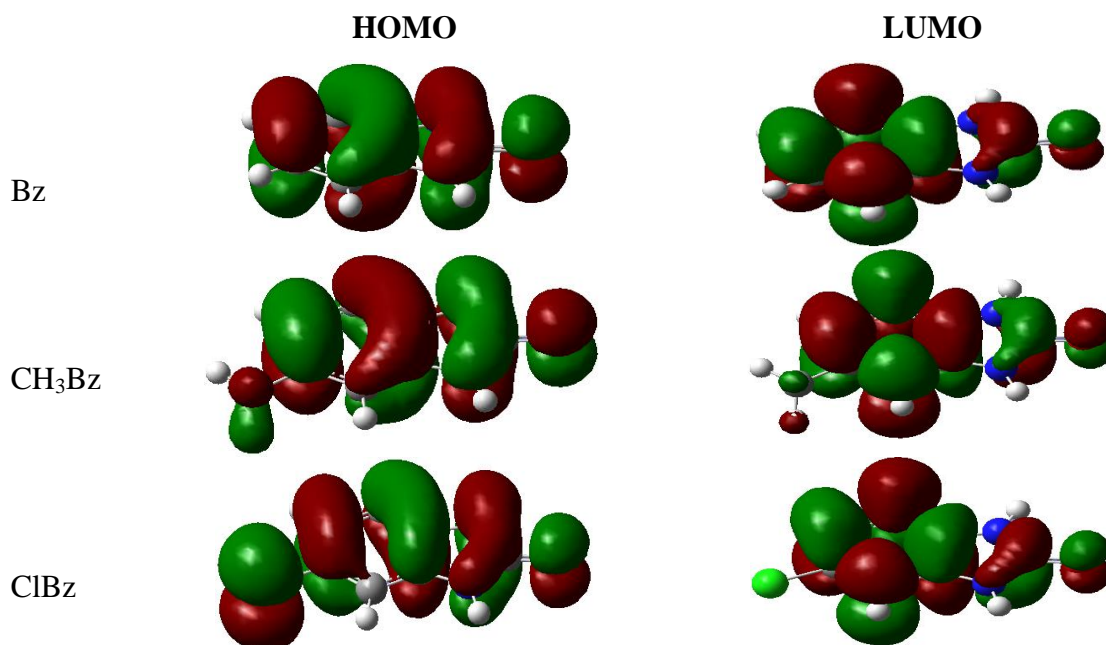
Isotropic polarizability <α> and anisotropic polarizability (Δα) are given by:

$$\langle \alpha \rangle = \frac{1}{3} (\alpha_{xx} + \alpha_{yy} + \alpha_{zz}) \quad (5)$$

$$\Delta \alpha = \left( \frac{1}{2} \right)^{1/2} \left[ (\alpha_{xx} - \alpha_{yy})^2 + (\alpha_{xx} - \alpha_{zz})^2 + (\alpha_{yy} - \alpha_{zz})^2 + 6(\alpha_{xx}^2 + \alpha_{yy}^2 + \alpha_{zz}^2) \right]^{1/2} \quad (6)$$

where  $\alpha_{ii}$  are the components of the polarizability matrix, The MPP (minimum polarizability principle) was postulated [44], who expects that the evolution natural direction of any system is for a state of MP (minimum polarizability). The more stable species have the lowest sum of <α> in reactions [45-47], inversely; the most reactive species are those that have a high polarizability. The accumulated distribution of negative charges (TNC) is another important

factor that should be considered, the high TNC that is accumulated at adsorption centers, the high electrostatic interaction among them and charged metal surface, therefore, electron-rich molecules are easily released electrons to orbitals without iron occupancy [21,48,49].



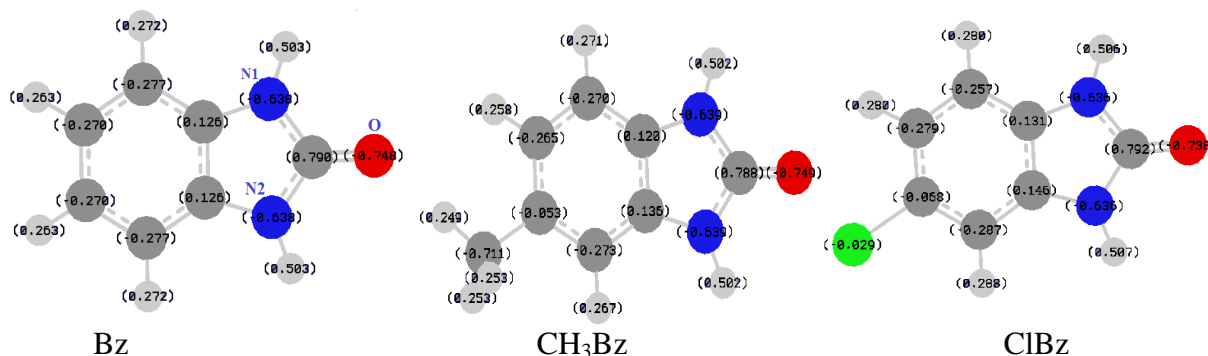
**Fig. 2.** Contour plots of HOMOs and LUMOs of (Bz), ( $\text{CH}_3\text{Bz}$ ) and ( $\text{ClBz}$ ) in the neutral form.

Table 1 shows that ( $\text{ClBz}$ ) has the highest value of the isotropic polarizability (158.55 u.a.) and anisotropic polarizability (139.77 u.a.), which probably increases its reactivity and increases the inhibition efficiency. It is clear from our results that ( $\text{ClBz}$ ) presents the highest molecular volume  $V_i$  (115.11  $\text{cm}^3/\text{mol}$ ), which increases contact area, thereby increasing its adsorption on the metal surface. However, dipole moment, total negative charges TNC and  $E_{\text{HOMO}}$ , which does not allow us to draw a clear correlation between them and the inhibitory potency of these molecules, leading us to make other calculations taking into account the effect of protonation.

The contour plots of the Kohn–Sham are shown in Fig. 2. From the figures, it may be considered that ( $\text{ClBz}$ ), ( $\text{CH}_3\text{Bz}$ ) and ( $\text{Bz}$ ) have similar HOMOs and LUMOs frontier orbitals electron density distributions. The HOMO orbitals are all located practically on the entire inhibitor moiety, especially located around the  $\text{C}=\text{C}$  and  $\text{C}=\text{N}$  moiety, and are also located on the 2Pz (27.90 %) atomic orbitals of the oxygen atom. However, LUMO orbitals are mainly localized on the ring of benzene fragments of inhibitors, more precisely, they are localized on the 2Pz atomic orbitals of C1 (25.70 %), C2 (25.70 %), C4 (22.64 %) and C5 (22.64 %).

### 3.2.2. Theoretical study of protonated inhibitors

Bz, CH<sub>3</sub>Bz and ClBz compounds are easily protonated to cationic forms in acidic solution due to the presence of nitrogen and oxygen atoms.



**Fig. 3.** Natural charges population analysis of Bz, CH<sub>3</sub>Bz and ClBz

It is shown from Fig. 2 that HOMOs frontier orbitals electron density distributions are localized practically on the entire inhibitor moiety (larger electronic density) indicating that, there are several active centers for the electrophilic attack, therefore, several probably sites upon the protonation for all inhibitors under study. The favorable protonation sites were revealed by the calculation of the PA as follows [21,47]:

$$PA = E_{\text{protonated}} - E_{\text{H}_3\text{O}^+} - E_{\text{neutral}} + E_{\text{H}_2\text{O}} \quad (7)$$

In this section, our investigation was limited to the nitrogen and oxygen atoms, seeing that as well as they have unshared electron pairs, have also, the highest values of the Natural charge Population Analysis (NPA) (see Fig.3). The NPA charges, total energy of protonated inhibitors and proton affinities (PA) are presented in Table 4. It is shown from this table that all values of the proton affinity are negative this means that all the inhibitors tend spontaneously to protonation in acidic medium. As a result of their elevated values of the proton affinity, the protonation at oxygen atom is favoured than at other heteroatoms, for example attaining (-4.421 eV) in the event of CH<sub>3</sub>Bz. By calculating the total energy, this result equals to (-24904.149 eV).

The theoretical parameters/descriptors of the protonated molecules calculated in aqueous phase are summarized in Table 4. Data analysis of this table shows a lowermost value of  $E_{\text{LUMO}}$  for ClBz (-1.387 eV) in comparison to CH<sub>3</sub>Bz (-1.167 eV) and Bz (-1.161 eV) which is in accordance with experimental inhibition efficiencies, demonstrating that these inhibitors have a strong ability to accept electrons from the occupied “d” orbitals of the metal.

**Table 4.** The calculated NPA charge densities of selected atoms, total energy and the proton affinities for protonated inhibitors

Compound	Center	NPA charge	Total energy (eV)	Proton affinity
Bz	N1	-0.638	-12397.203	-3.674
	N2	-0.638	-12397.203	-3.674
	O	-0.748	<b>-12397.937</b>	<b>-4.408</b>
CH <sub>3</sub> Bz	N1	-0.639	-13467.181	-3.711
	N2	-0.639	-13467.165	-3.695
	O	-0.749	<b>-13467.891</b>	<b>-4.421</b>
ClBz	N1	-0.636	-24903.401	-3.592
	N2	-0.636	-24903.354	-3.545
	O	-0.738	<b>-24904.149</b>	<b>-4.340</b>

The  $E_{\text{HOMO}}$  of this class increases in the order ClBz > CH<sub>3</sub>Bz > Bz. That is in good correlation with a ranking of inhibition efficiency obtained from electrochemical polarization method, proving that these inhibitors can offer electrons to metal surface. Also, ClBz has the smallest  $\Delta E = E_{\text{LUMO}} - E_{\text{HOMO}}$  (5.294 eV) compared with the other compounds. In addition, one might expect that ClBz molecule has a greater tendency to adsorb on metal surface than other compounds, which is a good correlation with experimental inhibition efficiency. These results are completely different from what we obtained in the case of the neutrals inhibitors.

Furthermore, Table 5 shown that the dipole moment ( $\mu$ ), isotropic polarizability  $\langle \alpha \rangle$ , and the anisotropic polarizability  $\Delta\alpha$  of the protonated inhibitors is in order: ClBz > CH<sub>3</sub>Bz > Bz which suggests that ClBz has the highest inhibition efficiency of the organic molecules studied, which is confirmed by the data obtained by experimentation.

It clearly appears that almost all the parameters calculated in the protonated form are strongly correlated with experimental inhibition efficiencies. In addition, the energies  $E_{\text{HOMO}}$  are clearly correlated with the corrosion inhibition efficiency, indicating that, this class of inhibitor compounds can adsorb on the mild steel surface based on D–A interactions among  $\pi$ -electrons of the aromatic ring or else among unshared electron pairs of hetero-atoms and vacant d-orbitals of surface iron atoms. Similarly, the energies  $E_{\text{LUMO}}$  are also strongly correlated with the experimental inhibition efficiency; this could lead to the conclusion that the strongest feedback bonds are formed in the case of the protonated inhibitors increasing

the chemical adsorption (chemisorptions) of inhibitor compounds on the steel surface.

**Table 5.** Calculated parameters for Bz, CH<sub>3</sub>Bz and ClBz in protonated form in aqueous phase

Quantum chemical properties	Bz	CH <sub>3</sub> Bz	ClBz
E <sub>HOMO</sub> (eV)	-6.946	-6.747	-6.681
E <sub>LUMO</sub> (eV)	-1.161	-1.167	-1.387
ΔE (eV)	5.785	5.580	5.294
μ (Debye)	7.232	8.617	13.728
V <sub>i</sub> (cm <sup>3</sup> /M)	101.79	106.63	87.25
< α > (u.a.)	129.10	145.08	147.57
Δα (u.a.)	101.79	109.36	127.59
TNC (e)	-2.851	-3.337	-2.649

### 3.2.3. The adsorption behavior of Benzimidazolone derivatives on iron surface

Two types of adsorption are known, chemisorption and physisorption. On the other side, physisorption results from electrostatic interactions among the charged centers of compounds and the charged metal surface, which results in a dipole interaction of compounds and metal surface. In order to present a model on the adsorption mechanism of organic compounds on the surface of the substrate, research was conducted on the inhibitor molecules adsorbed on an iron surface represented by an iron atom [50-53]. It is shown by Fig. 2 that there is one or more active centre on the inhibitor for adsorption, since, local reactivity/selectivity has been carried out by means of the Fukui indices [54,55], therefore, they indicate the reactive regions, in the form of the nucleophilic and electrophilic behaviour of each atom in the compounds.

The Fukui function  $f(\mathcal{R})$  is determined by [44,45]:

$$f(\mathcal{R}) = \left( \frac{\partial \rho(\mathcal{R})}{\partial N} \right)_{v(\mathcal{R})} \quad (8)$$

$\rho(\mathcal{R})$  : Electronic density, N: Number of electrons,  $v(\mathcal{R})$ : External potential;

- An electrophilic attack:

$$f^-(\mathcal{R}) = \left( \frac{\partial \rho(\mathcal{R})}{\partial N} \right)_{v(\mathcal{R})}^- \quad (9)$$

$$f_k^+(\beta) = \left( \frac{\partial \rho(\beta)}{\partial N} \right)_{\nu(\beta)}^+ \quad (10)$$

-A nucleophilic attack:

The condensed Fukui functions are defined by [56,57]:

$$f_k^- = P_k(N) - P_k(N-1) \quad (\text{For electrophilic attack}) \quad (11)$$

$$f_k^+ = P_k(N+1) - P_k(N) \quad (\text{For nucleophilic attack}) \quad (12)$$

**Table 6.** Fukui functions for protonated Bz, CH<sub>3</sub>Bz, and ClBz molecules

Molecule	Atoms	$P_k(N)$	$P_k(N+1)$	$P_k(N-1)$	$f_k^+$	$f_k^-$
Bz	C1	3.856	3.858	3.707	0.022	0.149
	C2	3.855	3.859	3.689	0.004	<b>0.166</b>
	C3	4.242	4.284	4.253	0.042	-0.011
	C4	4.235	4.265	4.106	0.030	<b>0.129</b>
	C5	4.235	4.264	4.073	0.029	<b>0.162</b>
	C6	4.241	4.284	4.259	0.043	-0.018
	C7	3.163	3.465	3.089	<b>0.302</b>	0.074
	N12	5.570	5.65	5.556	<b>0.080</b>	0.014
	N14	5.564	5.642	5.544	<b>0.078</b>	0.02
	O	6.671	6.798	6.584	<b>0.127</b>	0.087
CH <sub>3</sub> Bz	C1	3.847	3.868	3.758	0.021	<b>0.089</b>
	C2	3.862	3.876	3.695	0.014	<b>0.167</b>
	C3	4.235	4.415	4.219	<b>0.180</b>	0.016
	C4	4.231	4.287	4.127	0.056	<b>0.104</b>
	C5	4.020	4.066	3.834	0.046	<b>0.186</b>
	C6	4.239	4.423	4.225	<b>0.184</b>	0.014
	C7	3.164	3.284	3.101	<b>0.120</b>	0.063
	N11	5.571	5.592	5.560	0.021	0.011
	N13	5.564	5.588	5.535	0.024	0.029
	O	6.672	6.717	6.604	0.045	0.068
ClBz	C1	3.836	3.864	3.702	0.028	<b>0.134</b>
	C2	3.853	3.875	3.688	0.022	<b>0.165</b>
	C3	4.221	4.405	4.208	<b>0.184</b>	0.013
	C4	4.243	4.305	4.163	0.062	<b>0.080</b>
	C5	4.035	4.065	3.936	0.030	<b>0.099</b>
	C6	4.250	4.436	4.225	<b>0.186</b>	0.025
	C7	3.159	3.275	3.099	<b>0.116</b>	0.060
	N11	5.562	5.579	5.552	0.017	0.010
	N13	5.567	5.587	5.539	0.020	0.028
	O	6.667	6.713	6.599	0.046	0.068
	Cl	6.985	7.065	6.759	0.080	<b>0.226</b>

A high value of  $f_k^+$  indicates that the calculated atom gains electrons on reduction, therefore, can be the center of nucleophilic attack, and a high value of  $f_k^-$  show that the atom releases electrons when the compounds is oxidized, in addition, corresponds to reactivity with respect to electrophilic attack.

The Fukui functions for a nucleophilic and electrophilic attack and the corresponding population for the neutral and ionic species are given for the three selected inhibitors in Table 6 (for all atoms with the exception of the hydrogen). From this table, it is possible to be observed that in each one of the studied inhibitors, the C1, C2, C4 and C5 are the most appropriate sites for electrophilic attacks, seeing that, these sites present the highest  $f_k^-$ , which indicates that these sites are more able to give electrons to form coordinate bonds with the metal atoms. Regarding  $f_k^+$ , the largest values are observed at C3, C6 and C7 in CH<sub>3</sub>Bz and ClBz. In Bz inhibitors the largest  $f_k^+$  are observed at C7, N12, N14 and O which implied that these sites will be the nucleophilic reactive sites probably able to accept electrons from metal atoms and the strongest feedback bonds may be formed with the metal surface.

We use a simple modelling by simulating at first approach the interaction iron/molecule by calculating the combined energy by using the following equation [58,59]:

$$E_{com} = E_{(Fe-X)} - (E_{Fe} + E_X) \quad (13)$$

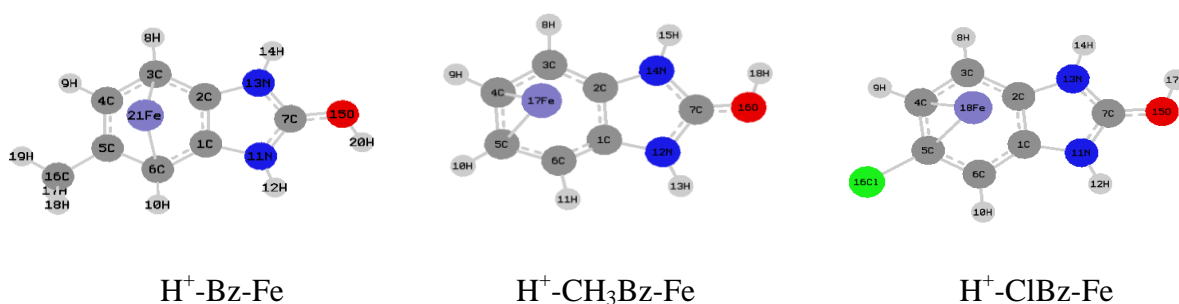


**Fig. 4.** Optimized molecular structures of Fe-inhibitor complexes

It is noted that the large  $E_{binding}$  value corresponds to the more stable formed complex. The optimized structures of the stable  $H^+$ -Bz-Fe,  $H^+$ -CH<sub>3</sub>Bz-Fe and  $H^+$ -ClBz-Fe complexes are shown in Fig. 4.

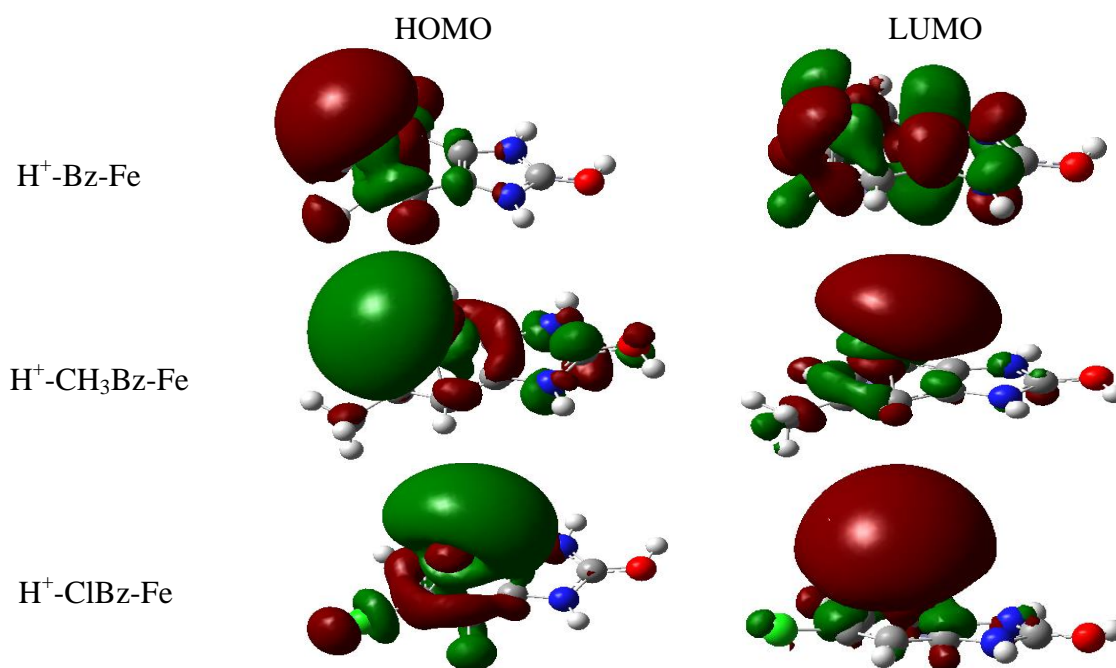


**Fig. 5.** Contour plots of HOMOs and LUMOs of ( $\text{H}^+$ -Bz-Fe), ( $\text{H}^+$ -CH<sub>3</sub>Bz-Fe) and ( $\text{H}^+$ -ClBz-Fe)

It is shown from the calculations that the  $\text{H}^+$ -Bz-Fe and  $\text{H}^+$ -ClBz-Fe complexes are formed when the inhibitor attacks the surface through  $\pi_{\text{C}_4=\text{C}_5}$ . The contour of the HOMO (Fig.5) demonstrates expecting strong  $\pi_{\text{C}_4=\text{C}_5}$  coordination to  $d_{x^2-y^2}$  iron orbital, upon which the extended Hückel calculations [60] shows that a large overlapping  $\langle \pi_{\text{C}_4=\text{C}_5} | d_{x^2-y^2} \rangle$  was occurred equal to 0.63 and 0.68 for  $\text{H}^+$ -Bz-Fe and  $\text{H}^+$ -ClBz-Fe complexes, respectively.

Concerning  $\text{H}^+$ -CH<sub>3</sub>Bz-Fe, the interaction was ensured through 2P<sub>Z</sub> orbitals of C3 and C6. By using another bonding analysis approach, NBO (Natural Bond Orbital) [61,62], we found a good overlapping of  $\langle \text{Fe} | \text{C3} \rangle$  and  $\langle \text{Fe} | \text{C6} \rangle$  equal to 0.667 and 0.744, respectively, and an orbital electronic occupation of Fe–C3 and Fe–C6 equal to 1.810 and 1.861, respectively. Starting from the shape of the LUMO(s) orbitals, a strong overlap can take place via a feedback effect from metal to ligand (Fig. 5).

Combined energy ( $E_{\text{com}}$ ) as well as thermochemistry investigated values obtained from a frequency calculation in (298.150 K, 1.00 Atm) such as the adsorption free energy ( $\Delta G_{\text{ads}}^\circ$ ), for Fe-inhibitors complex are given in Table 7. Both of these parameters were computed to compare the energetic and thermochemistry behavior of all possible adsorption sites. We observed in Table 7 that all  $E_{\text{com}}$  and  $\Delta G_{\text{ads}}^\circ$  values is negative, which means that the

combination and consequently the adsorption is an exothermic process, and could occur spontaneously.

The most relevant results of the adsorption free energy and combined energy that ClBz makes it possible to form the stable complex.

The binding energy values were also computed (Table 6), which is the negative combined energy value,  $E_{binding} = E_{com}$  [63]. The binding energies of  $H^+$ -ClBz-Fe complex equal to 242.992 kJ/mol, which is higher than the  $H^+$ -Bz-Fe, and  $H^+$ -CH<sub>3</sub>Bz-Fe compounds. It is well known that the higher binding energy. Thus, the calculated results may justify why ClBz was considered experimentally as a better corrosion inhibitor in the studied family.

It generally accepted that the  $\Delta G_{ads}^\circ$  less negative than (-20 KJ mol<sup>-1</sup>) be obtained for the mechanism of physisorption, while the values around or more negative than (-40 KJ mol<sup>-1</sup>) expected for the mechanism of chemisorption. From our calculations (see table 5, 4th column), the values of  $\Delta G_{ads}^\circ$  range from -226.908 to -249.105 (kJ mol<sup>-1</sup>) which clearly indicates that chemical adsorption is involved.

**Table 7.** The combined energies ( $E_{com}$  in kJ/mol), the binding energies ( $E_{binding}$  in kJ/mol) and the free energy of combination ( $\Delta G_{com}^\circ$  in kJ/mol) for the protonated surfactant-iron complexes

Complex	$E_{com}$	$E_{binding}$	$\Delta G_{ads}^\circ$
$H^+$ -Bz-Fe	-222.827	222.827	-226.908
$H^+$ -CH <sub>3</sub> Bz-Fe	-226.477	226.477	-232.643
$H^+$ -ClBz-Fe	<b>-242.992</b>	<b>242.992</b>	<b>-249.105</b>

### 3.3. Molecular dynamic simulations

#### 3.3.1. Interaction and adsorption properties with the influence of temperature of an inhibitory molecule on the Fe(110) surface

In the present work, our objective is studied influence of the temperature on the adsorption behavior of the chemical species existing within the supercell namely the corrosive ions ( $H_3O^+$ ,  $Cl^-$ ), water molecules and inhibitor mentioned.

As already referred in the literature, the temperature is very important parameters that allow destroying the bonds of an electrostatic nature formed between the atoms of an inhibitor and the atoms of a metal surface [64].

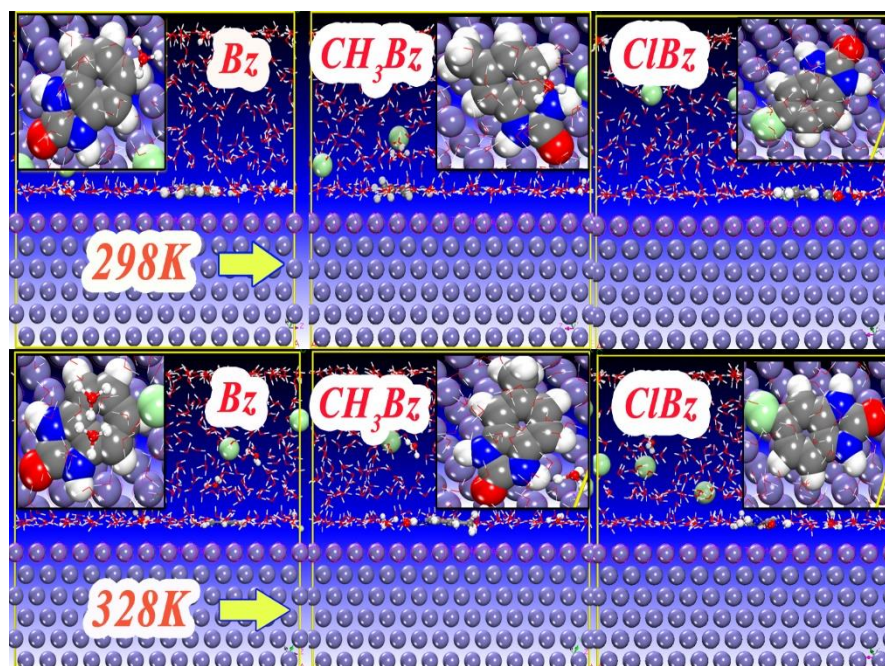


**Fig. 6.** Equilibrium adsorption configurations of Bz, CH<sub>3</sub>Bz and ClBz inhibitors on Fe (110) surfaces in the acid medium (HCl) with temperatures simulated 298 and 328 K

After the equilibrium, the most stable adsorption configurations for three Benzimidazolone derivatives adsorbed on Fe (110) surfaces for two temperatures simulated such as 298 and 328 K are shown in Fig. 6. The side and top views of the representations of the most stable configurations given in this figure show that Bz, CH<sub>3</sub>Bz and ClBz inhibitors are adsorbed just above the first layer of metal in parallel despite the increase of the temperature. This indicates that the investigated inhibitors also inhibit corrosion with the high temperature of 328 K. In addition, the increase in temperature affects the distribution of Cl<sup>-</sup> and H<sub>2</sub>O<sup>+</sup> corrosive ions within the solution. The competition of adsorption between the water molecules and the monomer of the inhibitor on the metal surface can decrease the corrosion inhibition performance [65].

The system studied now is in equilibrium, the energy fluctuation curves such as kinetic energy, non-bond energy, total energy and potential energy with temperatures simulated 298 and 328 K are shown in Fig. 7. It's clearly remarked that the system studied is in equilibrium at the end of the MD simulation process.

After the systems studied in case of equilibrium, the minimum values of the interaction energies ( $E_{\text{interaction}}$ ) and the maximum values of the binding energies ( $E_{\text{binding}}$ ) and its variations as a function of two simulated temperatures are collected in Table 7. The comparison between  $E_{\text{interaction}}$  values for the three inhibitors Bz, CH<sub>3</sub>Bz and ClBz for two temperatures 298 and 328 K shows that the ClBZ compound has a minimum value of the  $E_{\text{interaction}}$  and a high value of the  $E_{\text{binding}}$ . This means that this inhibitor has higher interaction

and adsorption performance on the metal surface than the CH<sub>3</sub>Bz and Bz. Thus, the results grouped in Table 8 show that the increase in temperature leads to a decrease in the adsorption efficiency of the inhibitors under study, this behavior is due to the increase in the values of the interaction energies. These findings confirm the results obtained experimentally.

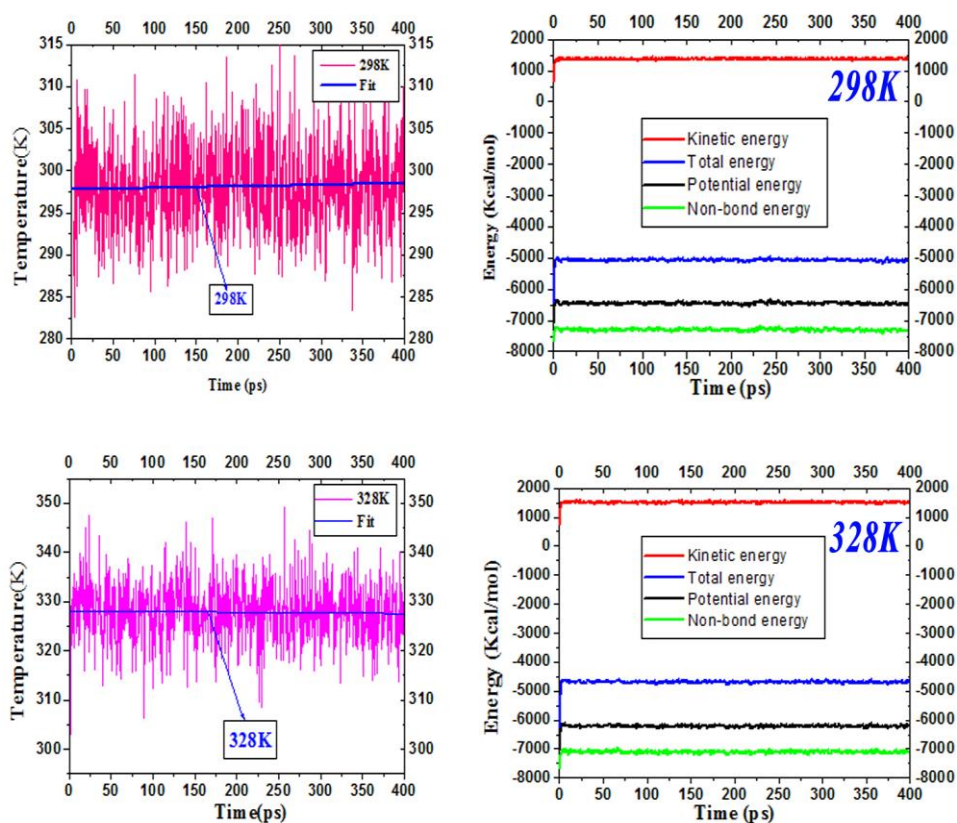


**Fig. 7.** Energy fluctuation and temperature curves obtained for system studied at 298 and 328 K

**Table 8.**  $E_{\text{interaction}}$  and  $E_{\text{binding}}$  energies with temperatures (298 and 328 K) for the three inhibitors Bz, CH<sub>3</sub>Bz and ClBz adsorbed on Fe (110) surfaces, all values in kJ mol<sup>-1</sup>

Inhibitor	T = 298 K		T = 328 K	
	$E_{\text{interaction}}$	$E_{\text{binding}}$	$E_{\text{interaction}}$	$E_{\text{binding}}$
Bz	-583.567	583.567	-500.458	500.458
ClBz	-612.821	612.821	-573.015	573.015
CH <sub>3</sub> Bz	-591.932	591.932	-560.236	560.236

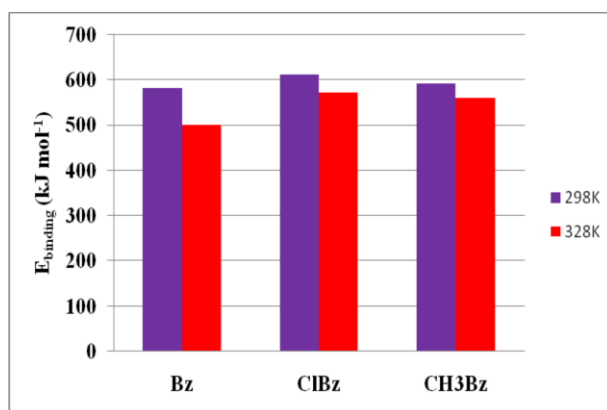


**Fig. 8.** Variation of  $E_{\text{binding}}$  as a function of the simulated temperatures for Bz, CH<sub>3</sub>Bz and ClBz

### 3.3.2. RDF functions

In this section, the radial distribution functions (RDFs) has been used as a useful method for calculating the distance between atoms of an inhibitor and metal.

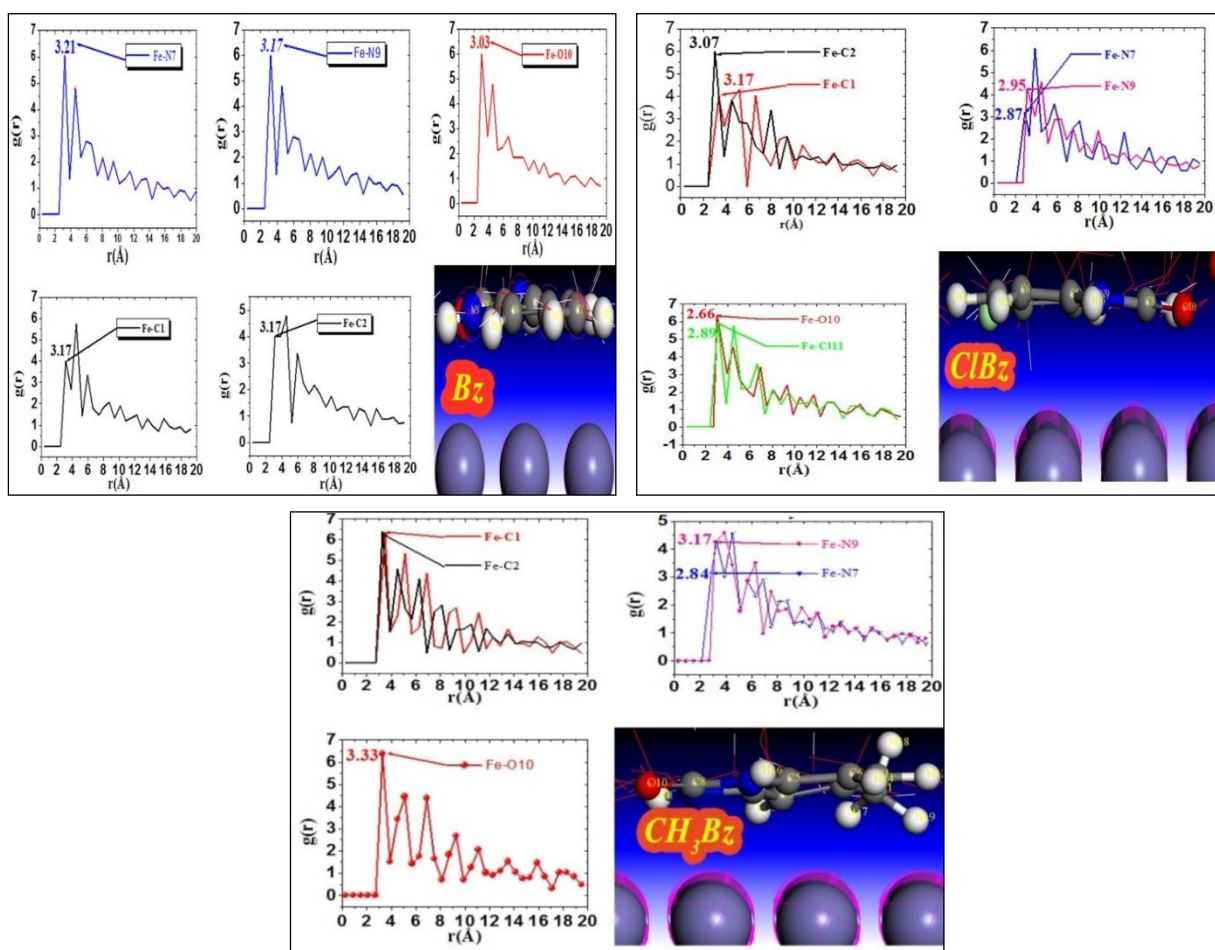


**Fig. 9.** Bond lengths such as iron-oxygen ( $g_{\text{Fe-O}}$ ), iron-carbon ( $g_{\text{Fe-C}}$ ), iron-nitrogen ( $g_{\text{Fe-N}}$ ) and iron-chlorine ( $g_{\text{Fe-Cl}}$ ) RDFs of the simulated systems at 298 K

The results grouped in Fig. 8 shows that the increase in temperature leads to the diminution of  $E_{binding}$ . The high value of  $E_{binding}$  of ClBz compound shows that this inhibitor has a better ability to adsorb on the iron surface. The values of  $E_{binding}$  are decreased when the temperature increases, it shows that the adsorption efficiency of these inhibitors is decreased. ClBz keeps its highest adsorption property on the metal substrate despite increasing temperature such as  $E_{binding}(ClBz) > E_{binding}(CH_3Bz) > E_{binding}(Bz)$ .

RDFs are defined as the finding probability of a pair of particles (A and B) at a distance  $r$  apart, relative to the expected probability for an entirely random distribution of the same density. In addition,  $\langle \rho_B \rangle$  means the species density of B averaged over all shells around A species. It is given in the following form [66]:

$$g_{AB}(r) = \frac{1}{\langle \rho_B \rangle_{local}} \times \frac{1}{N_A} \sum_{i \in A} \sum_{j \in B} \frac{\delta(r_{ij} - r)}{4\pi r^2} \quad (14)$$

The adsorption performance is generally related to bonds established between the atoms of a molecular structure and the atoms of the metal surface. The determination of the inhibitory / metal interactions is based on the nature of these bond lengths, noting that if the values are situated in the range of 1 Å -3.5 Å, then the coordination bonds exist [67]. The structure of inhibitors (Bz, CH<sub>3</sub>Bz and ClBz) and Fe(110) surfaces in the MD simulation systems can be Presented by intermolecular distances such as iron-oxygen ( $g_{Fe-O}$ ), iron-carbon ( $g_{Fe-C}$ ), iron-nitrogen ( $g_{Fe-N}$ ) and iron- chlorine( $g_{Fe-Cl}$ ) RDFs. The values noted in the curves of Fig. 9 are lower than 3.5 Å, which reflects that the nature of the bond lengths is coordinations (chemisorptions).

**Table 9.** Behavior of Bond lengths RDFs of the simulated systems at 298 and 328 K

Inhibitors	Bz		CH <sub>3</sub> Bz		ClBz	
	298 K	328 K	298 K	328 K	298 K	328 K
$g_{Fe-Cl}$	3.17	3.21	3.25	3.27	3.07	3.07
$g_{Fe-C2}$	3.17	3.15	3.09	3.19	3.17	3.27
$g_{Fe-C3}$	2.99	3.01	2.79	3.25	2.69	3.09
$g_{Fe-C4}$	3.09	3.05	3.13	3.25	2.95	3.25
$g_{Fe-C5}$	3.21	3.22	3.19	3.25	2.79	3.13
$g_{Fe-C6}$	2.89	3.01	2.85	3.25	3.05	3.13
$g_{Fe-N7}$	3.21	3.32	2.83	3.05	2.87	2.99
$g_{Fe-C8}$	3.21	3.25	3.15	3.03	2.69	3.27
$g_{Fe-N9}$	3.17	3.25	3.17	3.09	2.95	3.19
$g_{Fe-O10}$	3.03	3.09	3.33	3.34	2.53	2.93
$g_{Fe-Cl}$	—	—	—	—	2.89	3.15
$g_{Fe-C11}$	—	—	2.99	3.30	—	—

As we know that the increase in temperature affects the intramolecular bonds formed between the active sites of an inhibitor and vacant sites of the metal surface. In this new study, we are interested to monitor the behavior of the lengths of binding when they are subjected to an increase in temperature. Table 9 looks like all values of bond length inhibitor/metal systems simulated in 298 and 328 K. The results are grouped in Table 9 show that the increase in temperature leads to slightly spread the bonds lengths for the three inhibitors, but these values always remain in the chemisorption interval. Which reflects the performance of adsorption of these inhibitors on the surface of the steel is very high despite the increase in temperature. In addition, the values of the intramolecular bonds ClBz/Fe(110) are minimal compared to Bz/Fe(110) and CH<sub>3</sub>Bz/Fe(110). This shows that ClBz is better adsorbed on the surface of steel.

### 3.3.3. MSD simulation

The use of the mean squared displacement (MSD) to enhance the anticorrosive performance of each inhibitor studied in a super cell contains corrosive ions. For this purpose, we used a supercell containing 30 monomers of each inhibitor, 3Cl<sup>-</sup> and 3 H<sub>3</sub>O<sup>+</sup>. This model was used to calculate the diffusion coefficient (D) As follows:

$$D = \frac{1}{6N_{\alpha}} \lim_{x \rightarrow \infty} \frac{d}{dt} \sum_{i=1}^{N_{\alpha}} \langle [R_i(t) - R_i(0)]^2 \rangle \quad (15)$$

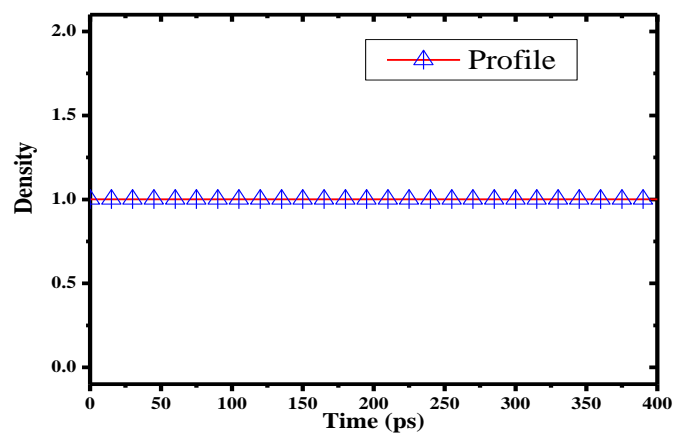
$N_{\alpha}$  describes the number of diffusive atoms, while  $R_i(0)$  and  $R_i(t)$  translates the positions of corrosive ions at the origin time (0) and a later time(t), respectively.

The migration rate of corrosive ions for each monomer of molecule is obtained from the MSD curves using equation (16) [68]:

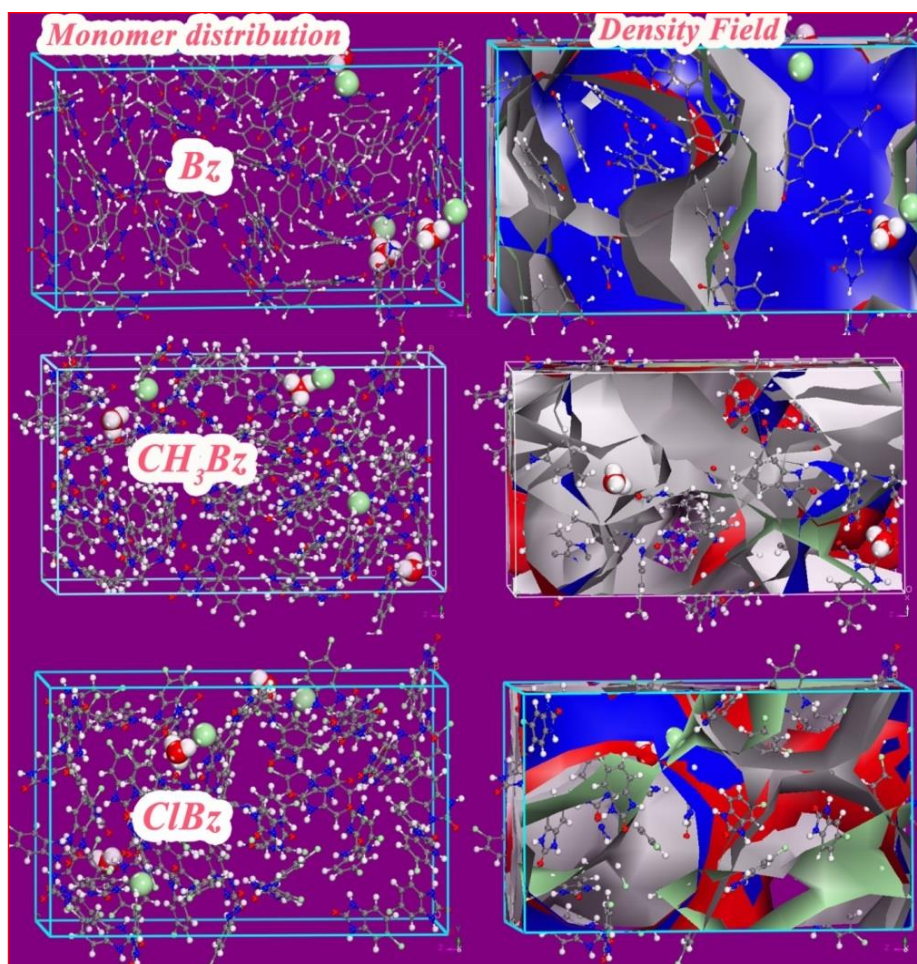
$$MSD = \langle [R_i(t) - R_i(0)]^2 \rangle \quad (16)$$

Fig. 10 describes the stability of the systems (supercells) studied, from this figure, the curve of the density profile is a horizontal line which stabilizes in a value which is equal to one of the density during the evolution of time. Indeed, this result shows that all the configurations presented in the Fig. 10 are in balance.

Fig. 11 shows density distributions and density field of the inhibitor and corrosive ion (Cl<sup>-</sup> and H<sub>3</sub>O<sup>+</sup>) monomers in a supercell. This model is essentially used to calculate the diffusion coefficient (D) (see Fig. 12 and Table 10) of the ions diffusing in the acidic medium HCl. According the findings observed in Fig. 11, it is very obvious that the supercell containing ClBz monomers is denser. This shows that this inhibitor has a better inhibitory efficiency.



**Fig. 10.** Density profile with the evolution of time of the systems studied in stable state



**Fig. 11.** MSD curves and the diffusion of ions of the studied ions in the Bz/CH<sub>3</sub>Bz /ClBz molecules at 298 K

The diffusion coefficient (D) is a very important parameter which makes it possible to

decrease the diffusion capacity of the ions studied. A minimal value of  $D$  indicates a large diffusion capacity of a chemical species [69]. From Fig. 12, it is possible to calculate  $D$  values. The latter for the  $\text{H}_3\text{O}^+$  and  $\text{Cl}^-$  ions for the two simulated temperatures 298 and 328 K are summarized in Table 10. The review of these results, we find that the minimum values of  $D$  for corrosive ions for the monomer ClBz reflect better inhibitory power. In addition, the increase in temperature leads to the increase of diffusion coefficient. This implies that the studied ions rapidly diffuse in particular the ion of  $\text{H}_3\text{O}^+$  because its mobility is very high compared to that of  $\text{Cl}^-$  ion, which leads to the lowering of the inhibitory efficiency of the monomers studied.

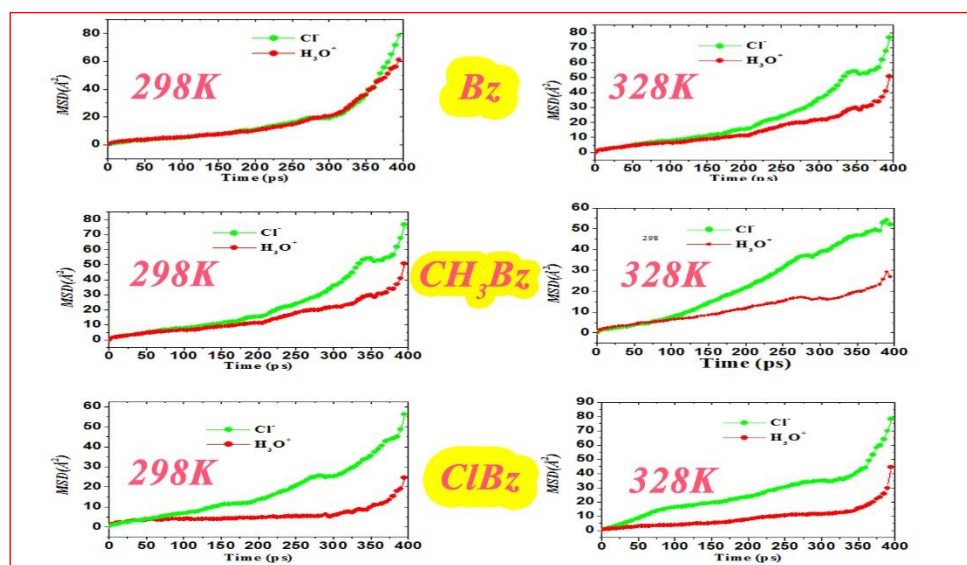


**Fig. 12.** MSD curves of diffusion of corrosive ions in presence of Bz,  $\text{CH}_3\text{Bz}$  and ClBz molecules at 298 and 328 K

**Table 10.** Diffusion coefficient values of  $\text{Cl}^-$  and  $\text{H}_3\text{O}^+$  ions in the supercell with Bz/ $\text{CH}_3\text{Bz}$  / ClBz in  $10^{12} \text{ m}^2 \text{ s}^{-1}$

Corrosive ion	$\text{Cl}^-$		$\text{H}_3\text{O}^+$	
	298 K	328 K	298 K	328 K
Bz monomer	0.12326	0.1543	0.1251	0.1284
$\text{CH}_3\text{Bz}$ monomer	0.09607	0.1187	0.0984	0.1199
ClBz monomer	0.05307	0.1095	0.1003	0.1105

### 3.4. MC simulations

The MC simulation was performed under the same conditions of MD simulation such as ours system containing 5 H<sub>3</sub>O<sup>+</sup>, 5 Cl<sup>-</sup>, 500 H<sub>2</sub>O and one monomer of molecules mentioned.

The binding ( $E_{\text{binding}}$ ) and adsorption ( $E_{\text{adsorption}}$ ) energies are calculated according to the following two equations [70,71].

$$E_{\text{adsorption}} = E_{\text{total}}(\text{system}) - (E_{\text{Fe}_{110}} + E_{\text{inhibitor}} + E_{5\text{Cl}^-} + E_{5\text{H}_3\text{O}^+} + E_{500\text{H}_2\text{O}}) \quad (17)$$

$$E_{\text{binding}} = -E_{\text{adsorption}} \quad (18)$$

The data of the MC simulations for the three systems studied listed in Table 11. The energy values grouped in Table 11 describe the studied systems, hence the degree of stability of these systems.  $E_{\text{adsorption}}$  values are negative for three systems studied, indicating that Bz, CH<sub>3</sub>Bz and ClBz are better adsorbed on the surface of the iron [72].

**Table 11.** Results obtained by MC simulations for adsorption of Bz, CH<sub>3</sub>Bz and ClBz on Fe (110) surfaces

Energies (kJ/mol)	Fe (110)- ClBz	Fe (110)- CH <sub>3</sub> Bz	Fe (110)- Bz
$E_{\text{adsorption}}$	-498.194	-490.850	-412.458
$E_{\text{binding}}$	498.194	490.850	412.458

The most negative value of  $E_{\text{adsorption}}$  (-498.194 kJ/mol) and more positive of  $E_{\text{binding}}$  (498.194 kJ/mol) of ClBz shows that this inhibitor has a higher adsorption performance. Therefore, the binding performance ( $E_{\text{binding}}$ ) between the products used and the Fe (110) surfaces is classed in the following order ClBz > CH<sub>3</sub>Bz > Bz.

The results obtained by MC simulations are comparable with those found by chemical quantum descriptor calculations and MD simulations. So, the methods used in this work very reliable.

## 4. CONCLUSION

From the results obtained in this work we can conclude that there is a very good agreement between theoretical and experimental results. Nearly all the parameters calculated in the neutral and in protonated form are strongly indicate that ClBz is the best inhibitors, which is in correlation with experimental data. All inhibitors studied tend spontaneously to protonation in acidic medium and the protonation at oxygen atom is favored than at other heteroatoms. The protonated form of inhibitors should make a higher contribution to the

corrosion inhibition effect of the inhibitors on ordinary steel. The binding energies of inhibitor molecules to the iron surface were estimated by one iron atoms. This involves a covalent bond between vacant d-orbitals of iron atoms and the  $\pi_{C=C}$  electrons of benzene ring and/or through  $2P_z$  orbitals of carbon atoms are involved. The adsorption process of Benzimidazolone derivatives is exothermic and could occur spontaneously. The results of thermochemistry based on a frequency calculation such as  $\Delta G_{ads}^\circ$  are indicative of a chemical adsorption (chemisorption). MD and MC simulations indicate that the compounds studied in this article are more efficient, and ClBz behaves as the best inhibitor in this Benzimidazolone series. The increase in temperature affects the binding energy and the interactions between the investigated inhibitors and the metal surface.

### Acknowledgment

The Hassan II Academy of Science and Technology have supported this work.

### REFERENCES

- [1] D. Ben Hmamou, R. Salghi, A. Zarrouk, H. Zarrok, B. Hammouti, S. S. Al-Deyab, A. El Assry, N. Benchat, and M. Bouachrine, *Int. J. Electrochem. Sci.* 8 (2013) 11526.
- [2] A. El Assry, B. Benali, B. Lakhri, M. El Faydy, M. Ebn Touhami, R. Tourir, and M. Touil, *Res. Chem. Intermed.* 41 (2015) 3419.
- [3] F. Benhiba, Y. ELaoufir, M. Belayachi, H. Zarrok, A. El Assry, A. Zarrouk, B. Hammouti, E. E. Ebenso, A. Guenbour, S. S. Al Deyab, and H. Oudda, *Der Pharm. Lett.* 6 (2014) 306.
- [4] M. Larouj, Y. ELaoufir, H. Serrar, A. El Assry, M. Galai, A. Zarrouk, B. Hammouti, A. Guenbour, A. El Midaoui, S. Boukhriss, M. Ebn Touhami, and H. Oudda, *Der Pharm. Lett.* 6 (2014) 324.
- [5] D. Ben Hmamou, R. Salghi, A. Zarrouk, H. Zarrok, R. Touzani, B. Hammouti, and A. El Assry, *J. Environ. Chem. Eng.* 3 (2015) 2031.
- [6] H. Tayebi, H. Bourazmi, B. Himmi, A. El Assry, Y. Ramli, A. Zarrouk, A. Geunbour and B. Hammouti, *Der Pharm. Chem.* 6 (2014) 220.
- [7] H. Tayebi, H. Bourazmi, B. Himmi, A. El Assry, Y. Ramli, A. Zarrouk, A. Geunbour, B. Hammouti, and E. E. Ebenso, *Der Pharm. Lett.* 6 (2014) 20.
- [8] H. Tayebi, B. Himmi, Y. Ramli, A. Zarrouk, A. Geunbour, A. Bellaouchou, H. Zarrok, M. Boudalia, and A. El Assry, *Res. J. Pharm., Biol. Chem. Sci.* 6 (2015) 1861.
- [9] M. Belayachi, H. Serrar, H. Zarrok, A. El Assry, A. Zarrouk, H. Oudda, S. Boukhris, B. Hammouti, Eno E. Ebenso, and A. Geunbour, *Int. J. Electrochem. Sci.* 10 (2015) 3010.
- [10] M. Hosseini, S.F.L. Mertens, M. Ghorbani, M. R. Arshadi, *Mater. Chem. Phys.* 78 (2003) 800.

- [11] M. Belayachi, H. Serrar, A. El Assyry, H. Oudda, S. Boukhris, M. Ebn Touhami, A. Zarrouk, B. Hammouti, Eno E. Ebenso, and A. El Midaoui, *Int. J. Electrochem. Sci.* 10 (2015) 3038.
- [12] P. Lowmunkhong, D. Ungthararak, and P. Sutthivaiyakit, *Corros. Sci.* 52 (2010) 30.
- [13] F. Bentiss, C. Jama, B. Mernari, H. E. Attari, L. El Kadi, M. Lebrini, M. Traisnel, and M. Lagrenee, *Corros. Sci.* 51 (2009) 1628.
- [14] L. B. Tang, X. Li, L. Li, G. Mu, and G. Liu, *Surf. Coat. Technol.* 201 (2006) 384.
- [15] M. Lashkari, and M. R. Arshadi, *J. Chem. Phys.* 299 (2004) 131.
- [16] S. Bilgic, and N. Caliskan, *J. Appl. Electrochem.* 31 (2001) 79.
- [17] Z. Lazar, B. Benali, K. Elblidi, M. Zenkouar, B. Lakhrissi, M. Massoui, B. Kabouchi, and C. Cazeau-Dubroca, *J. Mol. Liq.* 106 (2003) 89.
- [18] B. Benali, Z. Lazar, K. Elblidi, B. Lakhrissi, M. Massoui, A. Elassyry, and C. Cazeau-Dubroca, *J. Mol. Liq.* 128 (2006) 42.
- [19] L.F. Pacios, Z. Lazar, and B. Benali, *J. Mol. Struct. (Theochem)* 594 (2002) 89.
- [20] B. Benali, A. El Assyry, A. Boucetta, Z. Lazar, and B. Lakhrissi, *Res. Chem. Intermed.* 41 (2015) 821.
- [21] M. Alamgir, D.S.C. Black, N. Kumar, Springer, Berlin, Heidelberg, 9 (2007) 87.
- [22] R. Paramashivappa, P. Phani Kumar, P.V. Subba Rao, A. Srinivasa Rao, *Bioorg. Med. Chem. Lett.* 13 (2003) 657.
- [23] M. Touil, N. Hajjaji, D. Sundholm, and H. Rabaâ, *Int. J. Quantum. Chem.* 113 (2013) 1365.
- [24] N. O. Obi-Egbedi, I. B. Obot, and M. I. El-Khaiary, *J. Mol. Struct.* 1002 (2011) 86.
- [25] A. D. Becke, *J. Chem. Phys.* 98 (1993) 5648.
- [26] M. J. Frisch, G. W. Trucks, H. B. Schlegel, G. E. Scuseria, M. A. Robb, and et al., *Gaussian 98, Revision A.6*, Gaussian, Inc., Pittsburgh, PA (2003).
- [27] M. Rbaa, F. Benhiba, I.B. Obot, H. Oudda, I. Warad, B. Lakhrissi, and A. Zarrouk, *J. Mol. Liq.* 276 (2019) 120.
- [28] M. Khattabi, F. Benhiba, S. Tabti, A. Djedouani, A. El Assyry, R. Touzani, I. Warad, H. Oudda, and A. Zarrouk, *J. Mol. Struct.* 1196 (2019) 231.
- [29] Materials Studio, Revision 8.0, Accelrys Inc., San Diego, USA (2015).
- [30] H.C. Andersen, *J. Chem. Phys.* 72 (1980) 2384.
- [31] H. Sun, *J. Phys. Chem. B* 102 (1998) 7338.
- [32] R. Hsissou, O. Dagdag, S. About, F. Benhiba, M. Berradi, M. El Bouchti, A. Berisha, and N. Hajjaji, *J. Mol. Liq.* 284 (2019) 182.
- [33] Y. Tang, F. Zhang, S. Hu, Z. Cao, Z. Wu, W. Jing, *Corros. Sci.* 74 (2013) 271.
- [34] E. Gutiérrez, J.A.Rodríguez, J. Cruz-Borbolla, J.G. Alvarado-Rodríguez, P. Thangarasub, *Corros. Sci.* 108 (2016) 23.
- [35] Al. Dutta, S.Kr. Saha, U. Adhikari, P. Banerjee, D. Sukul, *Corros. Sci.* 123 (2017) 256.

- [36] H. A. Sorkhabi, B. Shabani, B. Aligholipour, and D. Seifzadeh, *Appl. Surf. Sci.* 252 (2006) 4039.
- [37] G. Gece, and S. Bilgic, *Corros. Sci.* 51 (2009) 1876.
- [38] N. Khalil, *Electrochim. Acta.* 48 (2003) 2635.
- [39] J. Fang, J. Li, *J. Mol. Struct. (Theochem)* 593 (2002) 179.
- [40] Z. Zhou, and R. G. Parr, *J. Am. Chem. Soc.* 112 (1990) 5720.
- [41] G. Gece, *Corros. Sci.* 50 (2008) 2981.
- [42] A. Dwivedi, and N. Misra, *Der. Pharm. Chem.* 2 (2010) 58.
- [43] X. Li, S. Deng, H. Fu, and T. Li, *Electrochim. Acta* 54 (2009) 4089.
- [44] F. Kandemirli, M. Hoscan, A. Dimoglo, and S. Esen, *Phosphorus Sulfur.* 183 (2008) 1954.
- [45] U. Hohm, *J. Phys. Chem. A* 104 (2000) 8418.
- [46] Taner Arslan, Fatma Kandemirli, Eno E. Ebenso, Ian Love, and H. Alemu, *Corros. Sci.* 51 (2009) 35.
- [47] M.S. Masouda, M.K. Awad, M.A. Shaker, and M. M. T. El-Tahawy, *Corros. Sci.* 52 (2010) 2387.
- [48] S. E. Nataraja, T. V. Venkatesha, H. C. Tandon, and B. S. Shylesha, *Corros. Sci.* 53 (2011) 4109.
- [49] Z. El Adnani, M. Mcharfi, M. Sfaira, M. Benzakour, A. T. Benjelloun, M. Ebn Touhami, B. Hammouti, and M. Taleb, *Int. J. Electrochem. Sci.* 7 (2012) 6738.
- [50] R. M. Issa, M. K. Awad, and F. M. Atlam, *Appl. Surf. Sci.* 255 (2008) 2433.
- [51] D. X. Wang, and H. M. Xiao, *J. Mol. Sci.* 16 (2000) 102.
- [52] D. Turcio-Ortega, T. Pandiyan, J. Cruz, and E. Garcia-Ochoa, *J. Phys. Chem. C* 111 (2007) 9853.
- [53] E. Jamalizadeh, S. M. A. Hosseini, and A. H. Jafari, *Corros. Sci.* 51 (2009) 1428.
- [54] P. W. Ayers, and R. G. Parr, *J. Am. Chem. Soc.* 122 (2000) 2010.
- [55] W. Yang, and W. J. Mortier, *J. Am. Chem. Soc.* 108 (1986) 5708.
- [56] M. Abreu-Quijano, M. Palomar-Pardavé, A. Cuán, M. Romero-Romo, G. Negrón-Silva, R. Álvarez-Bustamante, A. Ramírez-López, and H. Herrera-Hernández, *Int. J. Electrochem. Sci.* 6 (2011) 3729.
- [57] P. W. Ayers, and M. Levy, *Theor. Chem. Acc.* 103 (2000) 353.
- [58] G. Bereket, C. Ogretir, and A. Yurt, *J. Mol. Struct. (Theochem)* 571 (2001) 139.
- [59] M. Sahin, G. Gece, F. Karcı, and S. Bilgiç, *J. Appl. Electrochem.* 38 (2008) 809.
- [60] R. Hoffmann. *J. Chem. Phys.* 39 (1963) 1397 and 40 (1964) 2474.
- [61] M. J. Frisch, J. A. Pople, et al., *Gaussian 03, Revision C.02*, Gaussian Inc., Wallingford CT, 2004.
- [62] K. A. Barakat, T. R. Cundari, and M. A. Omary, *J. Am. Chem. Soc.* 125 (2003) 14228.
- [63] S. Xia, M. Qui, L. Yu, F. Lui, and H. Zhao, *Corros. Sci.* 50 (2008) 2021.

- [64] F. Benhiba, N. Lotfi, K. Ourrak, Z. Benzekri, H. Zarrok, A. Guenbour, S. Boukhris, A. Souizi, M. El Hezzat, I. Warad, R. Tourir, A. Zarrouk, and H. Oudda, *J. Mater. Environ. Sci.* 8 (2017) 3834.
- [65] F. Benhiba, Z. Benzekri, A. Guenbour, M. Tabyaoui, A. Bellaouchou, S. Boukhris, H. Oudda, I. Warad, and A. Zarrouk, *Recent Chin. J. Chem. Eng.* (2020) in press, doi.org/10.1016/j.cjche.2020.03.002.
- [66] P. Naeiji, F. Varaminian, and M. Rahmati, *J. Nat. Gas Sci. Eng.* 44 (2017) 122.
- [67] F. Benhiba, H. Serrar, R. Hsissou, A. Guenbour, A. Bellaouchou, M. Tabyaoui, S. Boukhris, H. Oudda, I. Warad, and A. Zarrouk, *Chem. Phys. Lett.* 743 (2020) 137181.
- [68] K.F. Yan, X.S. Li, Z.Y. Chen, B. Li, and C.G. Xu, *Mol. Simul.* 39 (2013) 251.
- [69] L.Y. Ding, C.Y. Geng, Y.H. Zhao, and H. Wen, *Mol. Simul.* 33 (2007) 1005.
- [70] Z. Rouifi, F. Benhiba, M. El Faydy, T. Laabaissi, H. About, H. Oudda, I. Warad, A. Guenbour, B. Lakhrissi, and A. Zarrouk, *Chem. Data Collect.* 22 (2019) 100242.
- [71] F. Benhiba, R. Hsissou, Z. Benzekri, M.E. Belghiti, A. Lamhamdi, A. Bellaouchou, A. Guenbour, S. Boukhris, H. Oudda, I. Warad, and A. Zarrouk, *J. Mol. Liq.* (2020) 113367.
- [72] K. Cherrak, F. Benhiba, N.K. Sebbar, E.M. Essassi, M. Taleb, A. Zarrouk, and A. Dafali, *Chem. Data Collect.* 22 (2019) 100252.